This article has been accepted for publication in a future issue of this journal, but has not been fully edited. Content may change prior to final publication. Citation information: DOI 10.1109/LWC.2020.3001916, IEEE Wireless Communications Letters

Outage Performance of Uplink NOMA in Land Mobile Satellite Communications

Sotiris A. Tegos, *Student Member, IEEE,* Panagiotis D. Diamantoulakis, *Senior Member, IEEE,* Junjuan Xia, Lisheng Fan, and George K. Karagiannidis, *Fellow, IEEE*

***Abstract*—Non-orthogonal multiple access (NOMA) can be efficiently used in land mobile satellite (LMS) communications in order to increase link availability, coverage and reliability. In this paper, we study -for first time in the literature- the outage performance of an uplink LMS system consisting of two terrestrial user nodes which perform NOMA in the uplink, with either successive interference cancellation or joint decoding at the satellite receiver. Closed-form expressions for the outage probability are derived for both cases assuming composite shadowed-Rician fading channels. Finally, numerical results and simulations validate the theoretical analysis.**

***Index Terms*—Land mobile satellite communications, NOMA, outage probability**

I. Introduction

Land mobile satellite (LMS) networks are an integral part of the fifth generation (5G) ecosystem, since 5G as a terrestrial network will still be affected by the limitations of land-based infrastructures, which currently cover less than 20 per cent of the world [1]. For example, individuals or fleets that work mostly in remote locations, or those who travel between urban and rural area a hybrid LMS/5G solution can ensure mobility and connectivity. The potential roles of satellite are acknowledged by the 5G ecosystem in a technical report of 3rd Generation Partnership Project (3GPP) [2]. Considering the increasing requirements of LMS networks in terms of connectivity and data rate, the impact of channel fading, which depends on several factors, such as height, positioning of the buildings/trees, and weather conditions, and the utilized multiple access control scheme on performance are of paramount importance.

On the other hand, non-orthogonal multiple access (NOMA) can increase spectral efficiency, reliability and the number of connected users in future wireless networks. A comprehensive description of the NOMA techniques can be found in [3] and references therein. Specifically, in uplink NOMA more than one users transmit their signal in the same orthogonal block (time slot, frequency, etc) and, thus, multiuser detection techniques, such as successive interference cancellation (SIC) or joint decoding (JD), are used at the receiver to decode the user's message. In more detail, if SIC is used, a signal is decoded considering the other signals as interference, while in JD, all users' signals are jointly decoded to achieve the capacity region of both Gaussian and fading multiple access channels.

Recently, NOMA has been investigated as a promising access technique for LMS networks, since it has the potential to mitigate the impact of both multipath and shadow fading on the users' performance. More specifically, in [4], the downlink of an LMS network with NOMA was introduced and studied. Also, in [5], [6], the outage performance of an amplify-and-forward hybrid satellite-terrestrial relay networks with NOMA is investigated, where a satellite communicates with multiple terrestrial users through the help of a relay through NOMA. Furthermore, the downlink transmission of a NOMA-based integrated terrestrial-satellite network, in which the terrestrial networks and the satellite cooperatively provide coverage for ground users, while reusing the entire bandwidth is investigated in [7]. Finally, in [8], the impact of imperfect SIC of a downlink NOMA-based satellite networks is studied and the corresponding outage probability is derived.

In contrast to all the aforementioned research works that focused on the downlink, in the present contribution, the uplink of an LMS network with NOMA is considered. It should be highlighted that the concept of uplink is different from that of downlink NOMA, since in the uplink NOMA interfering messages are received form different nodes, i.e., via different links, while, as it has already been mentioned, any decoding order can be used at the receiver, which make the analysis particularly challenging. More specifically, closed-form expressions for the outage probability, when either SIC or JD is used to mitigate the interference at the receiver, are derived for composite shadowed-Rician fading channels. The special case of the line-of-sight (LoS) component following the Rayleigh distribution is also considered as an upper bound of the system's performance. In this case, simple closed-form expressions for the outage probability are derived, which provide useful insights for the system design.

II. System and Channel Model

A. System Model

We consider a LMS network consisting of a satellite node (SN) and two terrestrial user nodes (UNs), which perform NOMA in the uplink. Specifically, the UNs communicate in the same resource block (e.g. time slot) with the SN and the last performs either SIC or JD to decode both signals. We further assume that both UNs and the SN are equipped with a single antenna and the UNs are located at different positions in the ground, but they are served by the same SN [4].

S. A. Tegos and G. K. Karagiannidis are with Wireless Communication Systems Group (WCSG), Department of Electrical and Computer Engineering, Aristotle University of Thessaloniki, 54 124, Thessaloniki, Greece (e-mails: {tegosoti, geokarag}@auth.gr).

P. D. Diamantoulakis J. Xia, and L. Fan are all with the School of Computer Science, Guangzhou University, Guangzhou 510006, China (e-mails: padiaman@ieee.org, xiajunjuan@gzhu.edu.cn, lsfan@gzhu.edu.cn).

The research work of S. A. Tegos was supported by the Hellenic Foundation for Research and Innovation (HFRI) under the HFRI PhD Fellowship grant (Fellowship Number: 1394).

The corresponding author of this paper is L. Fan.

This work was supported in part by the NSFC under Grant 61871139, in part by the International Science and Technology Cooperation Projects of Guangdong Province (Application No. 906225517102), by the Science and Technology Program of Guangzhou under Grant 201807010103, and in part by the research program of Guangzhou University (No. YK2020008).

Assuming that i-th and j-th UNs have transmitted the signals x_i and x_j, the received signal at the SN is given by

$$y = \sqrt{p_i} h_i x_i + \sqrt{p_j} h_j x_j + n, \tag{1}$$

where p_k with $k \in \{i, j\}$, h_k and n denote the transmitted power of the k-th UN, the small scale fading coefficient of the link between the k-th UN and the SN and the additive white Gaussian noise (AWGN), respectively.

Assuming that SIC is used at the SN, the achievable rate of the i-th UN, if its signal is decoded first and considering the interference from the j-th UN's signal, is given by

$$R_{i,1} = \log_2 \left(1 + \frac{\gamma_i}{\gamma_j + 1} \right), \tag{2}$$

where $\gamma_k = \frac{p_k |h_k|^2}{\sigma^2}$ and σ^2 being the variance of the noise. If the i-th UN's signal is decoded second, considering the decoding result of the j-th UN's signal, the achievable rate is given by

$$R_{i,2} = \log_2 \left(1 + \frac{\gamma_i}{\epsilon \gamma_j + 1} \right), \tag{3}$$

where $\epsilon \in \{0, 1\}$ represents the decoding result of the UN's message that is decoded first. Moreover, assuming that JD is utilized, the achievable rate region is defined by the inequalities

$$\begin{aligned} R_k &\leq \log_2 (1 + \gamma_k) \\ R_i + R_j &\leq \log_2 (1 + \gamma_i + \gamma_j). \end{aligned} \tag{4}$$

B. Channel Model

Regarding the channels between the UNs and the SN, we assume that they undergo independent and identically distributed (i.i.d.) shadowed-Rician fading, which can efficiently describe the LMS channel characteristics. The two statistical models for the LMS link are described in [9] and [10]. In [9], the amplitudes of the scatter and the LoS follow Rayleigh and lognormal distributions, respectively, but the derived expressions are particularly complicated, whereas in [10], the Nakagami-m distribution is used to model the amplitude of the LoS instead of the lognormal distribution and the model fits well to the LMS link experimental data. Therefore, adopting the model described in [10], the composite shadowed-Rician distribution can be approximated with high accuracy through a distribution, resulting from the Rayleigh and the Nakagami-m distributions, with parameters (m, b, Ω) and probability density function (PDF) given by

$$f_{|h_k|^2}(x) = \alpha_k e^{-\beta_k x} {}_1F_1(m_k; 1; \delta_k x), \tag{5}$$

where $\alpha_k = \frac{1}{2b_k} \left(\frac{2b_k m_k}{2b_k m_k + \Omega_k} \right)$, $\beta_k = \frac{1}{2b_k}$, $\delta_k = \frac{\Omega_k}{2b_k (2b_k m_k + \Omega_k)}$, $2b_k$ and Ω_k denote the average power of the multipath and the line-of-sight (LoS) components, respectively, m_k is the parameter of the Nakagami-m distribution, and ${}_1F_1(\cdot;\cdot;\cdot)$ represents the confluent hypergeometric function [11]. To this end, it can be proved that the random variable γ_k, which expresses the received signal-to-noise ratio (SNR), also follows the same distribution with parameters $(m_k, \frac{p_k}{\sigma^2} b_k, \frac{p_k}{\sigma^2} \Omega_k)$. Hereinafter, α_k, β_k and δ_k are defined by the parameters of the random variable γ_k.

It should be highlighted that since the LMS channel undergoes block fading effect, it remains constant over the channelâs coherence time. Moreover, since satellite communication uses wideband signalling, each data pulse is extremely small, thus in each coherence time a large number of data symbols can be transmitted [12].

III. Outage Performance

A. Uplink NOMA with SIC

In this subsection, we derive a closed-form expression for the outage probability of the LMS NOMA system, when SIC is performed.

Theorem 1: The outage probability of the i-th UN, assuming that SIC is performed, is given in (6) at the top of the next page, where $\zeta_k = \beta_k - \delta_k$ and $\theta_k = 2^{\hat{R}_k} - 1$ with $\hat{R}_k$ being the target rate of the k-th UN,

$$c_1 = \begin{cases} \gamma \left(n + k_2 + 1, (\zeta_i \theta_i + \zeta_j) \frac{(\theta_i + 1)\theta_j}{1 - \theta_i \theta_j} \right), & \theta_i \theta_j < 1 \\ \Gamma (n + k_2 + 1), & \theta_i \theta_j \geq 1 \end{cases} \tag{7}$$

and c_2 is given in (8) at the top of the next page, with $\Gamma(\cdot)$, $\gamma(\cdot,\cdot)$, and $\Gamma(\cdot,\cdot)$ being the gamma function, the lower incomplete gamma function, and the upper incomplete gamma function, respectively [11].

Proof: The proof is provided in Appendix A. ∎

In the next proposition we present a simple closed-form expression for the outage probability, when $m_k = 1$, i.e., the amplitude of the LoS also follows the Rayleigh distribution. This expression is useful, because it provides a bound in the system's performance and allows useful insights to be extracted.

Proposition 1: The outage probability of the i-th UN for the special case of $m_k = 1$, assuming that SIC is performed, is given by

$$\begin{aligned} P_{ij}^{\mathrm{s}} = 1 &- e^{-\zeta_j \theta_j} - \frac{\alpha_j e^{-\zeta_i \theta_i}}{\zeta_i \theta_i + \zeta_j} c_3 \\ &+ \frac{\alpha_j e^{\zeta_i}}{\frac{\zeta_i}{\theta_j} + \zeta_j} c_4 + \frac{\alpha_i e^{-\zeta_j \theta_j}}{\zeta_i + \zeta_j \theta_j} \left(1 - e^{-(\zeta_i + \zeta_j \theta_j)\theta_i} \right), \end{aligned} \tag{9}$$

where

$$c_3 = \begin{cases} 1 - e^{-(\zeta_i \theta_i + \zeta_j) \frac{(\theta_i + 1)\theta_j}{1 - \theta_i \theta_j}}, & \theta_i \theta_j < 1 \\ 1, & \theta_i \theta_j \geq 1 \end{cases} \tag{10}$$

and

$$c_4 = \begin{cases} e^{-\left(\frac{\zeta_i}{\theta_j} + \zeta_j \right)\theta_j} - e^{-\left(\frac{\zeta_i}{\theta_j} + \zeta_j \right) \frac{(\theta_i + 1)\theta_j}{1 - \theta_i \theta_j}}, & \theta_i \theta_j < 1 \\ e^{-\left(\frac{\zeta_i}{\theta_j} + \zeta_j \right)\theta_j}, & \theta_i \theta_j \geq 1. \end{cases} \tag{11}$$

Proof: Setting $m_k = 1$ in (6), (9) is derived. It should be highlighted that in this case $\alpha_k = \zeta_k = \frac{p_k}{\sigma^2} (\Omega_k + 2b_k)$. ∎

An important insight that can be derived from (9) is the behavior of the outage probability in the high SNR regime, i.e., $\frac{p_k}{\sigma^2} \to \infty$.

This article has been accepted for publication in a future issue of this journal, but has not been fully edited. Content may change prior to final publication. Citation information: DOI 10.1109/LWC.2020.3001916, IEEE Wireless Communications Letters

$$P_{ij}^{\mathrm{s}} = \alpha_i\alpha_j \sum_{k_1=0}^{m_i-1}\sum_{k_2=0}^{m_j-1} \frac{(1-m_i)_{k_1}(1-m_j)_{k_2}(-\delta_i)^{k_1}(-\delta_j)^{k_2}}{k_1!k_2!\zeta_i^{k_1+1}\zeta_j^{k_2+1}} \left(\frac{\gamma\left(k_2+1,\zeta_j\theta_j\right)}{k_2!} - \frac{\gamma\left(k_1+1,\zeta_i\theta_i\right)}{k_1!}\right)$$
$$+ \alpha_i \sum_{k_1=0}^{m_i-1} \frac{(1-m_i)_{k_1}(-\delta_i)^{k_1}}{(k_1!)^2\zeta_i^{k_1+1}}\gamma\left(k_1+1,\zeta_i\theta_i\right) - \alpha_i\alpha_j \sum_{k_1=0}^{m_i-1}\sum_{k_1=0}^{m_j-1}\sum_{l=0}^{k_1}\sum_{n=0}^{l} \frac{(1-m_i)_{k_1}(1-m_j)_{k_2}(-\delta_i)^{k_1}(-\delta_j)^{k_2}}{k_1!(k_2!)^2 l!\zeta_i^{k_1+1}}$$
$$\times \binom{l}{n}\left(\frac{e^{-\zeta_i\theta_i}\left(\zeta_i\theta_i\right)^l}{(\zeta_i\theta_i+\zeta_j)^{n+k_2+1}}c_1 - e^{\zeta_i}\left(\frac{\zeta_i}{\theta_j}\right)^l(-\theta_j)^{l-n}c_2\right) + \alpha_i\alpha_j e^{-\zeta_j\theta_j}\sum_{k_1=0}^{m_i-1}\sum_{k_2=0}^{m_j-1}\sum_{l=0}^{k_2}\sum_{n=0}^{l}$$
$$\frac{(1-m_i)_{k_1}(1-m_j)_{k_2}(-\delta_i)^{k_1}(-\delta_j)^{k_2}}{(k_1!)^2k_2!l!\zeta_j^{k_2+1}}\binom{l}{n}\frac{\left(\zeta_j\theta_j\right)^l}{(\zeta_i+\zeta_j\theta_j)^{k_1+n+1}}\gamma\left(k_1+n+1,(\zeta_i+\zeta_j\theta_j)\theta_i\right)) \tag{6}$$

$$c_2 = \begin{cases} \sum_{p=0}^{n+k_2}\frac{p!}{\left(\frac{\zeta_i}{\theta_j}+\zeta_j\right)^{p+1}}\binom{n+k_2}{p}\left(e^{-\left(\frac{\zeta_i}{\theta_j}+\zeta_j\right)\theta_j}\theta_j^{n+k_2-p} - e^{-\left(\frac{\zeta_i}{\theta_j}+\zeta_j\right)\frac{(\theta_i+1)\theta_j}{1-\theta_i\theta_j}}\left(\frac{(\theta_i+1)\theta_j}{1-\theta_i\theta_j}\right)^{n+k_2-p}\right), & \theta_i\theta_j<1 \\ \left(\frac{\zeta_i}{\theta_j}+\zeta_j\right)^{-n-k_2-1}\Gamma\left(n+k_2+1,\left(\frac{\zeta_i}{\theta_j}+\zeta_j\right)\theta_j\right), & \theta_i\theta_j\geq 1 \end{cases} \tag{8}$$

$$P_{ij}^{\mathrm{c}} = \alpha_i \sum_{k_1=0}^{m_i-1}\frac{(1-m_i)_{k_1}(-\delta_i)^{k_1}}{(k_1!)^2\zeta_i^{k_1+1}}\gamma\left(k_1+1,\zeta_i\theta_i\right) + \alpha_j\sum_{k_2=0}^{m_j-1}\frac{(1-m_j)_{k_2}(-\delta_j)^{k_2}}{(k_2!)^2\zeta_j^{k_2+1}}\gamma\left(k_2+1,\zeta_j\theta_j\right)$$
$$+ \alpha_i\alpha_j\sum_{k_1=0}^{m_i-1}\sum_{k_2=0}^{m_j-1}\frac{(1-m_i)_{k_1}(1-m_j)_{k_2}(-\delta_i)^{k_1}(-\delta_j)^{k_2}}{k_1!(k_2!)^2\zeta_i^{k_1+1}\zeta_j^{k_2+1}}\left(\gamma\left(k_2+1,\zeta_j(\theta_i+1)\theta_j\right)\left(1-\frac{\gamma\left(k_1+1,\zeta_i\theta_i\right)}{k_1!}\right)\right. \tag{13}$$
$$\left. - \gamma\left(k_2+1,\zeta_j\theta_j\right)\right) - \alpha_i\alpha_j e^{-\zeta_i\theta_{ij}}\sum_{k_1=0}^{m_i-1}\sum_{k_2=0}^{m_j-1}\sum_{l=0}^{k_1}\sum_{n=0}^{l}\frac{(1-m_i)_{k_1}(1-m_j)_{k_2}(-\delta_i)^{k_1}(-\delta_j)^{k_2}}{k_1!(k_2!)^2l!\zeta_i^{k_1+1}}\binom{l}{n}(-\zeta_i)^l(-\theta_{ij})^{l-n}c_5$$

Proposition 2: The outage probability of the i-th UN for the special case of $m_k = 1$, assuming that SIC is performed, in the high SNR regime is given by

$$P_{ij}^{\mathrm{s},\infty} = \begin{cases} 0, & \theta_i\theta_j < 1 \\ \frac{\zeta_i\zeta_i(\theta_i\theta_j-1)}{(\zeta_i\theta_i+\zeta_j)(\zeta_i+\zeta_j\theta_j)}, & \theta_i\theta_j \geq 1. \end{cases} \tag{12}$$

Proof: Considering that $\frac{p_k}{\sigma^2}$ is contained in α_k and ζ_i and calculating the limits, (12) is derived. ∎

It should be highlighted that for the case of SIC a floor is observed in the outage performance of the considered system.

B. LMS Uplink NOMA with JD

In this subsection, we derive two closed-form expressions for the outage probability, assuming that JD is used to detect the UNs' messages at the BS, instead of SIC. More specifically, we derive the common outage probability which is defined as the probability that outage occurs in at least one of the UNs and the individual outage probability of the i-th UN where outage occurs in the i-th UN, regardless if outage occurs in the j-th UN or not [13].

Theorem 2: The common outage probability, assuming that JD is performed, is given in (13) at the top of this page, where $\theta_{ij} = (\theta_i+1)(\theta_j+1)-1$ and c_5 is given in (17) at the top of this page.

Proof: The proof is provided in Appendix B. ∎

Theorem 3: The individual outage probability of the i-th UN, assumming that JD is utilized, is given in (15) at the top of the next page.

Proof: The proof is provided in Appendix C. ∎

Accordingly with the previous subsection, the following propositions present the outage probability with JD for the case that the amplitude of the LoS also follows the Rayleigh distribution, which simplifies the derived expressions.

Proposition 3: The common outage probability, assuming that JD is performed, for the special case of $m_k = 1$ for both UNs is given by

$$P_{ij}^{\mathrm{c}} = 1 - e^{-\zeta_i\theta_i}e^{-\zeta_j(\theta_i+1)\theta_j} - \alpha_j e^{-\zeta_i\theta_{ij}}c_6, \tag{16}$$

where

$$c_6 = \begin{cases} \frac{1}{\zeta_i-\zeta_j}\left(e^{(\zeta_i-\zeta_j)(\theta_i+1)\theta_j} - e^{(\zeta_i-\zeta_j)\theta_j}\right), & \zeta_i\neq\zeta_j \\ \theta_i\theta_j, & \zeta_i=\zeta_j. \end{cases} \tag{17}$$

Proof: Setting $m_k = 1$ in (13), (16) is derived. ∎

Proposition 4: The individual outage probability of the i-th UN, assuming that JD is performed, for the special case of $m_k = 1$ for both UNs is given by

$$P_{ij}^{\mathrm{in}} = P_{ij}^{\mathrm{c}} - \frac{\alpha_j e^{-\zeta_i\theta_i}}{\zeta_i\theta_i+\zeta_j}\left(1-e^{-(\zeta_i\theta_i+\zeta_j)\theta_j}\right). \tag{18}$$

Proof: Setting $m_k = 1$ in (15), (18) is derived. ∎

This article has been accepted for publication in a future issue of this journal, but has not been fully edited. Content may change prior to final publication. Citation information: DOI 10.1109/LWC.2020.3001916, IEEE Wireless Communications Letters

$$c_5 = \begin{cases} \sum_{p=0}^{n+k_2} \frac{(-1)^p p!}{(\zeta_i-\zeta_j)^{p+1}} \binom{n+k_2}{p} \left(e^{(\zeta_i-\zeta_j)(\theta_i+1)\theta_j} \left((\theta_i+1)\theta_j\right)^{n+k_2-p} - e^{(\zeta_i-\zeta_j)\theta_j} \theta_j^{n+k_2-p} \right), & \zeta_i \neq \zeta_j \\ \frac{1}{n+k_2+1} \left(\left((\theta_i+1)\theta_j\right)^{n+k_2+1} - \theta_j^{n+k_2+1} \right), & \zeta_i = \zeta_j \end{cases} \tag{14}$$

$$P_{ij}^{\text{in}} = P_{ij}^{\text{c}} - \alpha_j \sum_{k_2=0}^{m_j-1} \frac{(1-m_j)_{k_2}(-\delta_j)^{k_2}}{(k_2!)^2 \zeta_j^{k_2+1}} \gamma\left(k_2+1, \zeta_j\theta_j\right) + \alpha_i\alpha_j \sum_{k_1=0}^{m_i-1} \sum_{k_2=0}^{m_j-1} \frac{(1-m_i)_{k_1}(1-m_j)_{k_2}(-\delta_i)^{k_1}(-\delta_j)^{k_2}}{k_1!(k_2!)^2 \zeta_i^{k_1+1} \zeta_j^{k_2+1}} \gamma\left(k_2+1, \zeta_j\theta_j\right)$$
$$+ \alpha_i\alpha_j e^{-\zeta_i\theta_i} \sum_{k_1=0}^{m_i-1} \sum_{k_2=0}^{m_j-1} \sum_{l=0}^{k_1} \sum_{n=0}^{l} \frac{(1-m_i)_{k_1}(1-m_j)_{k_2}(-\delta_i)^{k_1}(-\delta_j)^{k_2}}{k_1!(k_2!)^2 l! \zeta_i^{k_1+1}} \binom{l}{n} \frac{(\zeta_i\theta_i)^l}{(\zeta_i\theta_i+\zeta_j)^{k_2+n+1}} \gamma\left(k_2+n+1, (\zeta_i\theta_i+\zeta_j)\theta_j\right)) \tag{15}$$

In the high SNR regime, when JD is utilized, both the common and the individual outage probability is zero, which can be proved by calculating the limit of (16) as $\frac{p_k}{\sigma^2} \to \infty$. In the case of JD there is no floor in the outage performance, thus JD outperforms SIC in the high SNR regime.

IV. Simulations and Discussion

In this section, numerical results and simulations are provided to evaluate the outage performance of the considered system and validate the analytical results. We assume that one UN's link with the LMS undergoes frequent heavy shadowing (FHS) with $(m, b, \Omega) = (1, 0.063, 8.97 \times 10^{-4})$ and the other UN's link undergoes average shadowing (AS) with $(m, b, \Omega) = (10, 0.126, 0.835)$ and the thresholds are $\theta = 1$dB and $\theta = 3$dB, respectively. In the two figures the lines correspond to the theoretical results and the symbols correspond to the simulations.

In Fig. 1, the outage probability of the considered system is plotted versus the transmitted SNR of the UNs which is assumed to be the same for both UNs. For the case of JD the common outage performance is similar with the one of the UN with FHS, since this UN faces worse channel conditions. Also, it can be observed that JD outperforms SIC in the medium and high SNR regime and the floor in the outage performance of SIC is evident. The outage performance of the UN with AS is better for both SIC and JD, since the channel conditions are more favorable. Similar behavior is observed in Fig. 2 which illustrates the outage performance of a LMS network consisting of two UNs with FHS. In this case, $m = 1$ and the simple derived expressions for the outage probability are used. It is noticed that JD always outperforms SIC at the expense of increased complexity and as expected the performance is worse compared to the one illustrated in Fig. 1. In both figures a performance upper bound (PUB) is illustrated, where a resource block is used solely by one UN. It is obvious that this case is an upper bound in the performance, however when JD is utilized the achieved performance is close to this bound.

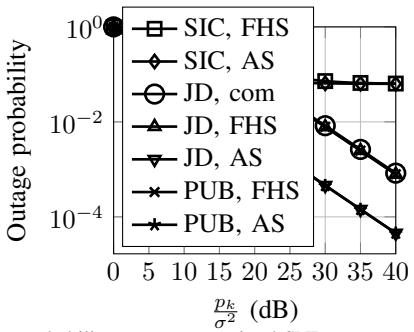

Fig. 1. Outage probability versus transmitted SNR.

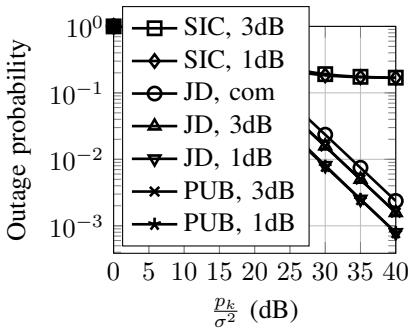

Fig. 2. Outage probability versus transmitted SNR for the special case of $m = 1$.

Appendix A
Proof of Theorem 1

Outage occurs in the i-th UN, regardless if outage occurs in the j-th UN or not, thus the outage probability of the i-th UN is given by [14]

$$P_{ij}^{\text{s}} = \Pr\left(\frac{\gamma_i}{\gamma_j+1} < \theta_i, \frac{\gamma_j}{\gamma_i+1} < \theta_j \right) + \Pr\left(\frac{\gamma_j}{\gamma_i+1} \geq \theta_j, \gamma_i < \theta_i \right). \tag{19}$$

Using the random variables $X = \gamma_i$ and $Y = \gamma_j$, the first term in (19), termed as P_1, can be written as

$$P_1 = \Pr\left(\frac{Y}{\theta_j} - 1 < X < \theta_i \left(Y+1\right) \right). \tag{20}$$

Considering that the expressions $\frac{X}{Y+1} = \theta_i$ and $\frac{Y}{X+1} = \theta_j$ intersect at the point $\frac{(\theta_i+1)\theta_j}{1-\theta_i\theta_j}$ if $\theta_i\theta_j < 1$, and they do not intersect if $\theta_i\theta_j \geq 1$, and that X and Y are independent, (20) can be rewritten as

$$P_1 = \int_0^d F_X\left(\theta_i\left(y+1\right)\right) f_Y(y) dy - \int_{\theta_j}^d F_X\left(\frac{y}{\theta_j} - 1\right) f_Y(y) dy, \tag{21}$$

This article has been accepted for publication in a future issue of this journal, but has not been fully edited. Content may change prior to final publication. Citation information: DOI 10.1109/LWC.2020.3001916, IEEE Wireless Communications Letters

where

$$d = \begin{cases} \frac{(\theta_i+1)\theta_j}{1-\theta_i\theta_j}, & \theta_i\theta_j < 1 \\ \infty, & \theta_i\theta_j \geq 1. \end{cases} \tag{22}$$

Assuming that m_w with $w \in \{i, j\}$ is a positive integer, the PDF of both X and Y can be written as

$$f_Z(z) = \alpha_w e^{-\zeta_w z} \sum_{k=0}^{m_w-1} \frac{(1-m_w)_k(-\delta_w)^k}{(k!)^2} z^k \tag{23}$$

with $Z \in \{X, Y\}$. Moreover, the CDF is given by

$$F_Z(z) = \alpha_w \sum_{k=0}^{m_w-1} \frac{(1-m_w)_k(-\delta_w)^k}{(k!)^2\zeta_w^{k+1}} \gamma(k+1, \zeta_w z). \tag{24}$$

Considering that the incomplete gamma function can be written as [11]

$$\gamma(k+1, z) = k!\left(1 - e^{-z}\sum_{l=0}^{k}\frac{z^l}{l!}\right) \tag{25}$$

and after some algebraic manipulations the two integrals in (21) can be calculated.

Furthermore, the second term in (19), termed as P_2, can be written as

$$P_2 = \Pr\left(\frac{Y}{X+1} \geq \theta_j, X < \theta_i\right). \tag{26}$$

Considering that X and Y are independent, (26) can be rewritten as

$$P_2 = \int_0^{\theta_i} \left(1 - F_Y\left(\theta_j(x+1)\right)\right) f_X(x)dx. \tag{27}$$

Following similar steps, the integral in (27) can be calculated and (6) can be derived.

Appendix B
Proof of Theorem 2

Utilizing JD, outage occurs when (θ_i, θ_j) is out of the capacity region, thus the common outage probability is given by

$$P_{ij}^{\mathrm{c}} = 1 - \Pr\left(\gamma_i \geq \theta_i, \gamma_j \geq \theta_j, \gamma_i + \gamma_j \geq \theta_{ij}\right). \tag{28}$$

Using the random variables $X = \gamma_i$ and $Y = \gamma_j$ which are independent, (28) can be rewritten as

$$P_{ij}^{\mathrm{jd}} = 1 - \int_{\theta_j}^{\infty} \Pr\left(X \geq \theta_i, X + y \geq \theta_{ij}\right) f_Y(y)dy. \tag{29}$$

In (29), the probability can be rewritten as

$$\Pr\left(X \geq \theta_i, X + y \geq \theta_{ij}\right) = 1 - F_X\left(\max\{\theta_i, \theta_{ij} - y\}\right), \tag{30}$$

where $\max$ denotes the maximum of the two elements. The second term in $\max$, $\theta_{ij} - y$, is greater than b_i, when $y < (\theta_i + 1)\theta_j$, thus (29) can be written as

$$\begin{aligned} P_{ij}^{\mathrm{jd}} = 1 &- \int_{\theta_j}^{(\theta_i+1)\theta_j} \left(1 - F_X\left(\theta_{ij} - y\right)\right) f_Y(y)dy \\ &- \int_{(\theta_i+1)\theta_j}^{\infty} \left(1 - F_X\left(\theta_i\right)\right) f_Y(y)dy. \end{aligned} \tag{31}$$

Following similar steps as in the proof of Theorem 1, (13) can be derived.

Appendix C
Proof of Theorem 3

Utilizing JD, the individual outage probability of the i-th UN is calculated by subtracting a term that indicates the probability that outage occurs in the j-th UN while the i-th UN is successfully decoded from the common outage probability and, thus, is given by

$$P_{ij}^{\mathrm{in}} = P_{ij}^{\mathrm{c}} - \Pr\left(\frac{\gamma_i}{\gamma_j + 1} \geq \theta_i, \gamma_j < \theta_j\right). \tag{32}$$

Using the random variables $X = \gamma_i$ and $Y = \gamma_j$, the subtracted term, P_{s} can be written as

$$P_{\mathrm{s}} = \Pr\left(X \geq \theta_i(Y+1), Y < \theta_j\right). \tag{33}$$

Considering that X and Y are independent, (33) can be rewritten as

$$P_{\mathrm{s}} = \int_0^{\theta_j} \left(1 - F_X\left(\theta_i(y+1)\right)\right) f_Y(y)dy. \tag{34}$$

Following similar steps as in the proof of Theorem 1, (15) can be derived.

References

[1] ESOA, "Satellite Communications Services: An integral part of the 5G Ecosystem (5G White Paper)," 2019.

[2] 3GPP, "TR 38.811: Study on New Radio (NR) to support non-terrestrial networks," 2017.

[3] Z. Ding, X. Lei, G. K. Karagiannidis, R. Schober, J. Yuan, and V. K. Bhargava, "A Survey on Non-Orthogonal Multiple Access for 5G Networks: Research Challenges and Future Trends," *IEEE J. Sel. Areas Commun.*, vol. 35, pp. 2181–2195, Oct. 2017.

[4] X. Yan, H. Xiao, C. Wang, K. An, A. T. Chronopoulos, and G. Zheng, "Performance Analysis of NOMA-Based Land Mobile Satellite Networks," *IEEE Access*, vol. 6, pp. 31327–31339, 2018.

[5] X. Yan, H. Xiao, C. Wang, and K. An, "Outage Performance of NOMA-Based Hybrid Satellite-Terrestrial Relay Networks," *IEEE Wireless Commun. Lett.*, vol. 7, pp. 538–541, Aug. 2018.

[6] X. Zhang, B. Zhang, K. An, Z. Chen, S. Xie, H. Wang, L. Wang, and D. Guo, "Outage Performance of NOMA-Based Cognitive Hybrid Satellite-Terrestrial Overlay Networks by Amplify-and-Forward Protocols," *IEEE Access*, vol. 7, pp. 85372–85381, 2019.

[7] X. Zhu, C. Jiang, L. Kuang, N. Ge, and J. Lu, "Non-Orthogonal Multiple Access Based Integrated Terrestrial-Satellite Networks," *IEEE J. Sel. Areas Commun.*, vol. 35, pp. 2253–2267, Oct. 2017.

[8] X. Yue, Y. Liu, Y. Yao, T. Li, X. Li, R. Liu, and A. Nallanathan, "Outage Behaviors of NOMA-based Satellite Network over Shadowed-Rician Fading Channels," *arXiv preprint arXiv:2003.03527*, 2020.

[9] Chun Loo, "A Statistical Model for a Land Mobile Satellite Link," *IEEE Trans. Veh. Technol.*, vol. 34, pp. 122–127, Aug. 1985.

[10] A. Abdi, W. C. Lau, M.-. Alouini, and M. Kaveh, "A New Simple Model for Land Mobile Satellite Channels: First- and Second-Order Statistics," *IEEE Trans. Wireless Commun.*, vol. 2, pp. 519–528, May 2003.

[11] I. S. Gradshteyn and I. M. Ryzhik, *Table of integrals, series, and products*. Academic press, 2014.

[12] M. N. Pachery and M. R. Bhatnagar, "Double Differential Modulation for LEO-Based Land Mobile Satellite Communication," *IEEE Trans. Aerosp. Electron. Syst.*, p. 1, 2020.

[13] R. Narasimhan, "Individual Outage Rate Regions for Fading Multiple Access Channels," in *Proc. IEEE Int. Symp. Information Theory*, pp. 1571–1575, Jun. 2007.

[14] M. Najafi, V. Jamali, P. D. Diamantoulakis, G. K. Karagiannidis, and R. Schober, "Non-Orthogonal Multiple Access for FSO Backhauling," in *Proc. IEEE Wireless Communications and Networking Conf. (WCNC)*, pp. 1–6, Apr. 2018.